Geomechanics and Engineering, *Vol. 17, No. 2 (2019) 145-156*
DOI: https://doi.org/10.12989/gae.2019.17.2.145

Energy-based evaluation of liquefaction potential of uniform sands

Yetis Bulent Sonmezer*

Department of Civil Engineering, Faculty of Engineering, Kirikkale University, 71450 Kirikkale, Turkey

(Received October 3, 2018, Revised January 2, 2019, Accepted January 10, 2019)

Abstract. Since behaviors of loose, dense, silty sands vary under seismic loading, understanding the liquefaction mechanism of sandy soils continues to be an important challenges of geotechnical earthquake engineering. In this study, 36 deformation controlled cyclic simple shear tests were performed and the liquefaction potential of the sands was investigated using three different relative densities (40, 55, 70%), four different effective stresses (25, 50, 100, 150 kPa) and three different shear strain amplitudes (2, 3.5, 5%) by using energy based approach. Experiments revealed the relationship between per unit volume dissipated energy with effective stress, relative density and shear strain. The dissipate energy per unit volume was much less affected by shear strain than effective stress and relative density. In other words, the dissipated energy is strongly dependent on relative density and effective stress. These results show that the dissipated energy per unit volume is very useful and may contain the non-uniform loading conditions of the earthquake spectrum. When multiple regression analysis is performed on experiment results, a relationship is proposed that gives liquefaction energy of sandy soils depending on relative density and effective stress parameters.

Keywords: liquefaction energy; cyclic simple shear test; relative density; effective stress; shear strain; sand

1. Introduction

It is well-known that repetitive shear stresses caused by earthquakes lead to different strains depending on the physical and engineering features of the soil, which gives rise to loss of strength. When the type and properties of soil are considered, this loss of strength causes to fairly exhibit different dynamic behaviors and stress-strain properties of soils under permanent loadings. Water-saturated loose sands in particular can lose their strength quickly since excess pore water pressure increases fast both in static and in dynamic loading conditions, which can severely damage to structural systems. These damages are observed in buildings as being buried in soil and tilting or lateral displacement of retaining structures or slopes (Towhata 2008). This type of behavior occurring in saturated sandy soils is called liquefaction, and it constitutes one of the more important and interesting topics in geotechnical earthquake engineering and soil dynamics.

Over the last decades, researchers have proposed different methods to better understand the liquefaction mechanism and to identify the liquefaction potential of soils. It is possible to consider these methods as three main groups (Green 2001): stress-based methods, strain-based methods, and energy-based methods.

Stress-based method (Seed and Idriss 1971) is the most commonly used method for evaluating liquefaction. Empirical data obtained from field test results and laboratory results are generally used in this method. However, the method has some uncertainties, such as earthquake magnitude, maximum horizontal ground acceleration, and source distance, and it is constantly updated with new studies (Youd *et al.* 1996). The basic criterion in this method is the number of cycles and the level of shear stress. Associating real earthquake motion with harmonic loading conditions in the laboratory requires the equivalent stress and number of cycles as defined in the method proposed by Seed and Idriss (1971). Seed *et al.* (1975) proposed that 65% of the maximum shear stress occured in 15 cycles of the permanent loading. Ishara and Yasuda (1975) offered to 57% for 20 cycles of the permanent loading, rather than 65%. Although the stress-based approach is constantly expanded and revised with the data of liquefaction cases, the uncertainties pertinent to random properties of given loading continued (Green 2001, Baziar and Jafarian 2007). Moreover, some approaches depending on field tests, such as standard penetration test (SPT) and cone penetration test (CPT), were developed to determine the liquefaction potential of a site (Çetin *et al.* 2004, Boulanger and Idriss 2012, Moss 2012).

The strain-based method was first proposed by Dobry *et al.* (1982). It was derived from the mechanics of two interacting idealized sand grains, and then it was generalized for natural soils (Baziar and Jafarian 2007, Alavi and Gandomi 2012, Green 2001). This method is mainly based on the hypothesis that pore water pressure initiates to develop when the shear strain surpasses a threshold shear strain of about 0.01% regardless of the type of sand, relative density, initial effective stress value and specimen preparation method. Although it is theoretically possible, a strain-based method is used less often because it estimates the point that the increase in pore water pressure must reach for liquefaction to occur. In addition, this situation does not necessarily mean that liquefaction will

*Corresponding author, Ph.D.
E-mail: bsonmezer@kku.edu.tr

http://www.techno-press.org/?journal=gae&subpage=7
ISSN: 2005-307X (Print), 2092-6219 (Online)

occur. The main drawback of this method is the difficulty of estimating shear strain compared to repetitive shear stress (Seed 1980, Zhang *et al.* 2015).

The energy-based approach was proposed for the first time in the 1970s as an alternative to the stress-based approach, in order to evaluate the liquefaction potential of soil (Nemat-Nasser and Shokooh 1979); it has been continuously developed ever since (Berrill and Davis 1985, Figueroa *et al.* 1994, Kokusho 2013, Green 2001). In this approach, whether or not liquefaction occurs, energy dissipated per unit volume is directly related to the development of excess pore water pressure during the loading process. Energy accumulated in the unit volume associated with permanent rearrangement of particles (J/m^3) is defined as the area in the hysteresis loop developed during a cycle. It is quite feasible to use unit energy to evaluate liquefaction, because liquefaction energy is completely dependent upon the applied shear stress and shear strain (Fardad Aminia and Noorzad 2018). Some experimental studies carried out to evaluate liquefaction energy per unit volume are summarized below.

Simcock *et al.* (1983) carried out a series of dynamic triaxial tests to explain the relation between excess pore water pressure in uniform sands and energy dissipated until the onset of liquefaction in the soil. They stated that a functional relationship exists between excess pore water pressure and dissipated energy, and that this relationship is strongly dependent on cyclic deviator stress. Towhata and Ishihara (1985) carried out a series of undrained tests on the Toyoura sand by using hollow torsional shear tests; they showed that a strong relationship exists between the energy dissipated per unit volume for the liquefaction of the soil and the excess pore water pressure at different shear stress values. Figueroa *et al.* (1994) carried out a series of tests on Reid Bedford sand by using hollow torsional shear test instruments, and they concluded that the energy per unit volume transferred to the soil to achieve liquefaction is related to the effective environmental stress and relative density; however, it is not related to shear strain. A similar conclusion was also reached in a study carried out by Liang (1995). Liang carried out a series of controlled strain tests with hollow torsional shear test instruments, and determined that shear strain amplitude has no effect on the relationship between the cumulative dissipated energy per unit volume for the onset of liquefaction and the excess pore water pressure.

The study carried out by Polito *et al*. (2013) examined the effect of different loading methods on the relationship between pore water pressure and energy dissipated until the onset of liquefaction on isotopically-consolidated sand specimens. For this purpose, they carried out a series of stress-controlled dynamic triaxial tests. In addition to sinusoidal loading (although the difference is not large in the number of loading cycles causing liquefaction of triangular square regular symmetric and irregular asymmetric different loading shapes), they stated that the energy accumulated per normalized unit volume at the onset of liquefaction does not depend on the loading shape, but rather depends on the loading rate. Jafarian *et al.* (2012) carried out a series of tests in undrained conditions by using the hollow torsional shear test in different relative density and stress conditions. They derived a new nonlinear equation from the test results, which showed that energy dissipated per unit volume for the onset of liquefaction based on initial effective stress and relative density. They stated that this equation worked well as a boundary curve for distinguishing facts from analyses carried out in the liquefied and non-liquefied fields.

Liquefaction energy per unit volume has been researched through numerical studies as well as experimental studies. Baziar and Jafarian (2007) applied the neural network procedure to laboratory test results to estimate the energy accumulated per normalized unit volume at the onset of liquefaction. They showed a consistency between energy accumulated in the unit volume obtained from both field observations and laboratory test results. Chen *et al.* (2005) proposed a model based on back-propagation neural networks and seismic wave energy to evaluate the potential of liquefaction. They indicated that the model gave consistent results regarding predictions of liquefaction energy. Nemat-Nasser and Shoko (1979) proposed a mathematical model explaining the liquefaction and compression of sandy soils by using the energy-based model. In another model proposed by Zhang and Goh (2016) using real field observation and test results, the modification of the Logistic Regression (LR) LR_MARS based Multivariate Adaptive Regression Spline (MARS) approach was used to assess the seismic liquefaction potential based on actual field records. The use of the LR_MARS model in seismic evaluation has been shown to be promising in determining liquefaction potential.

Compared to stress and strain-based approaches, the main advantages of energy-based approach in liquefaction analysis are as follows: 1) Energy is a scalar quantity, considering the whole spectrum of ground motion, in comparison with a stress-based approach, which only uses the peak value of ground acceleration (Baziar and Jafarian 2007, Baziar and Jafarian 2011). Temporal decomposition of shear stress is not required to find the number of cycles equivalent to the selected average stress or strain level. 3) The fact that its use involves both strain and stress, as well as material properties, can also be an advantage (Liang 1995, Law *et al*. 1990). During an earthquake, the soil amplifies ground motion in certain frequency ranges while absorbing in other frequency ranges. However, it has been reported that the total energy circulating and dispersed in the soil does not change in energy approach, regardless of whether part of the motion is amplified or absorbed (Law *et al*. 1990).

The energy associated with the rearrangement and settlement of sand particles during repetitive loading conditions is considered to be a fixed amount under specific conditions, causing liquefaction (Figueroa *et al.* 1994). A typical repetitive loading test provides stress, shear strain, and pore water pressure. The shear stress-shear strain hysteresis loop can be obtained as a function of time, as shown in Fig. 1. Cumulative dissipated energy in each loading cycle is equivalent to cumulative enclosed area of hysteresis loop in Fig. 1 (Ostadan *et al.* 1996, Zhang 2015, Green 2001). The energy in each cycle and the sum of these energies until the onset of liquefaction are defined as the liquefaction energy of soil (Alavi and Gandomi 2012). The relationship given in Eq. (1) is frequently used in literature

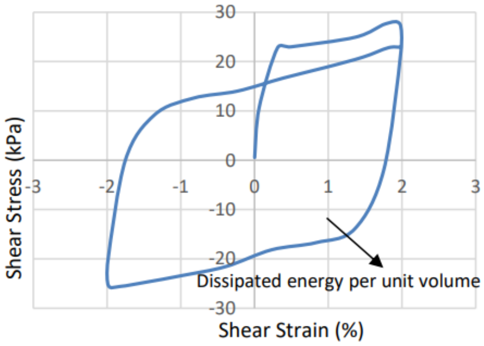

Fig. 1 Typical hysteresis loop under cyclic simple shear

when calculating the area within the typical hysteresis loop (Figueroa *et al.* 1994, Liang 1995).

$$\delta W = \frac{1}{2}\sum_{i=1}^{n}(\tau_n + \tau_{n+1})(\gamma_{n+1} - \gamma_n) \qquad (1)$$

where, τ = shear stress, γ = shear strain, and n = number of cycles recorded until liquefaction, δW: Cumulative total energy.

The energy dissipated for each cycle from 1st cycle to the nth cycle in which liquefaction occurs is calculated by using the formula above, and the total liquefaction energy (J/m^3) of the specimen is determined by adding these energies together.

In the literature, when studies related to liquefaction are examined, it can been seen that dynamic triaxial test, hollow cylinder torsional shear test, and cyclic simple shear test are most frequently used. The dynamic triaxial test cannot model field loading conditions correctly (Kammerer and Pestana 2002); however, the first analyses carried out by Seed and Lee (1967) showed that liquefaction data obtained from the triaxial test can be beneficial for evaluating the behavioral trends of a field. Nevertheless, since applied stress trace does not decently represent shear stresses spreading vertically in the soil profile, care should be taken when using this data to derive specific conclusions about general behavior (Kammerer and Pestana 2002). Although the hollow cylinder torsional shear test models field loading conditions well, it can cause redistribution of voids and a non-uniform cross-sectional area, due to a high surface area compared to specimen volume and non-uniform application of radial strain on the specimen and tall specimen height (Kammerer and Pestana 2002). Besides modeling field loading conditions well, the cyclic simple shear test has a relatively-uniform stress distribution in the active part of the specimen, because of the small specimen height (Monkul *et al.* 2015). Furthermore, in this test, consolidation is anisotropic (as in field conditions) and it can apply normal stress and horizontal shear stress on the test specimen. This characteristic of horizontal shear stress application is unique to cyclic simple shear test, and this characteristic separates it from the hollow cylinder torsional shear test (Kammerer and Pestana 2002). Compared to the other two mentioned tests, the cyclic loading mechanism in the cyclic simple shear test is more similar to earthquake loading conditions

The scope of this study is to test the liquefaction potential of a uniform sand under varying conditions of effective stresses and relative densities, using the strain-controlled cyclic simple shear, and to establish a relationship that predicts liquefaction energy as a function of effective stress and relative density.

2. Cyclic simple shear test and test arrangement

In the cyclic simple shear test, experiments can be carried out under “undrained” and “drained constant volume” conditions. In drained constant volume tests, since the height of the specimen does not change, the constant volume is maintained by adjusting the magnitude of effective stress on the specimen. Since drainage is provided during the test, excess pore water pressure does not occur; however, pore water pressure equivalent to that of the undrained test is estimated based on the change in vertical effective stress (Bjerrum and Landva 1966). In the undrained test, some researchers keep vertical stress constant during the test (Dyvik *et al.* 1987); some (Chang and Hong 2008, Hazirbaba and Rathje 2009, Jafarzadeh and Sadeghi 2012) keep the consolidation height of the specimen constant. Nevertheless, the specimen is tested in undrained conditions under any circumstances, and the produced excess pore water pressure is measured using precision pressure sensors. When the liquefaction of the soil is evaluated under laboratory conditions, the experiments can be carried out with stress control or strain control. Many researchers have carried out stress-controlled (Wijewichreme and Sriskandakumar 2005) and strain-controlled tests (Silver and Park 1976, Dobry *et al.* 1982) to examine the liquefaction potential of loose- and medium-dense sands. The determined cyclic shear stress is applied to the specimen in stress-controlled tests, and the strains cannot be controlled. In strain-controlled tests, however, the cyclic shear stress of the selected strain amplitude is applied on the soil specimen, and the developed excess pore water pressure is measured. Strain-controlled cyclic simple loading directly associates pore water pressure, and consequently the liquefaction, with shear strain amplitude (Talaganov 1996). This test models earthquake loading in the field more closely (Zaheer *et al.* 2013); thus, the strain-controlled test is preferred in this study.

The experiments in this study is carried out using a cyclic simple shear test instrument produced by Wille Geotechnik. In this device, loadings can be made in 1D, 2D, or 3D. While 1D and 2D loadings are made by pistons located on the right and left sides of the device, 3D loading is made on the device by means of a piston that stands in a vertical position, and this piston has the force application capacity of 10 kN. Loadings on the device can be sinusoidal or can be carried out as random loading by entering any displacement record of any earthquake. The view of the device used in the study is given in Fig. 2.

In saturated soils, a soil unit element at a certain depth is under both a geostatic total vertical stress (σ_V):and a hydrostatic pore water pressure (u_0)When such soil is exposed to repetitive loadings such as earthquakes besides hydrostatic pore water pressure, excess pore water pressure (Δu) starts to develop. When the sum of u_0 and Δu is equivalent to (σ_V), the soil is liquefied.

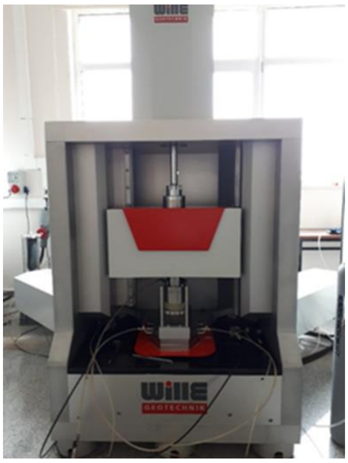

Fig. 2 Cyclic simple shear device used in this study

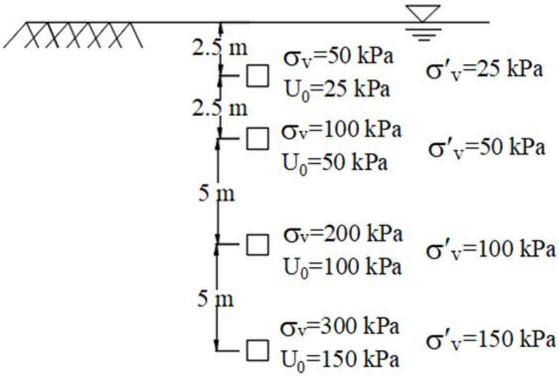

Fig. 3 Field initial conditions considered during experiment planning

Table 1 Properties of sand used in experiments

Property	Value
USCS classification symbol	SP
Median grain size, D50 (mm)	0.26
Specific gravity, Gs	2.65
Max. void ratio (emax)	0.852
Min. void ratio (emin)	0.571
Cu	1.75
Cc	0.89

When the experiment was planned, the initial conditions of the liquefiable layers in the field were generally taken into consideration, and the sand specimen was tested under these initial conditions. The study relied on the statement in recent studies that liquefaction was observed in the field layers whose depths are >10 m (Cubrinovski *et al.* 2013, Wotherspoon *et al.* 2015), as shown in Fig. 3. Thus, the geostatic vertical stress and hydrostatic pore water pressures at depths up to the first 15 m were taken into account in the experiments. When geostatic vertical stress (σ_V) and hydrostatic pore water pressure values (u_0) were being determined, the saturated unit weight was assumed to be $(\gamma_{sat})\cong 20$ kN/m^3, and the water unit volume weight was assumed to be (γ_w) 10 kN/m^3.

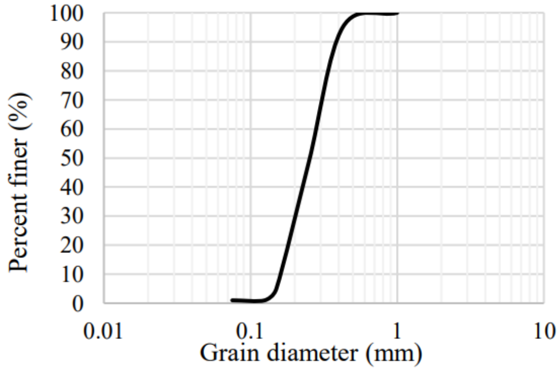

Fig. 4 Grain distribution curve of sand used in experiments

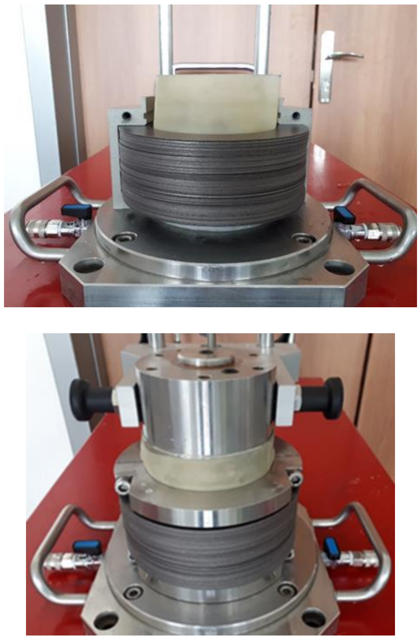

Fig. 5 Cyclic simple shear test mould limited by teflon-coated rings

In this study, 36 the strain-controlled undrained cyclic simple shear tests at strain values of 2, 3.5, 5%, were applied to the sand specimens at relative densities of 40, 55, 70% along with effective stress values 25, 50, 100, 150 kPa in order to determine the energy dissipated per unit volume at the onset of liquefaction. In some studies, it has been shown that the liquefaction energy of the soil under dynamic loading is little or no dependent on shear strain amplitude (Figuera *et al.* 1994, Liang 1995). Furthermore, in stress-controlled dynamic tests, it is assumed that the tested sample is liquefied when either the excess pore pressure is equal to the effective stress or when the shear strain amplitude reaches the double amplitude 6% or 10% (DeAlba et al 1976, Ishara 1985). Therefore, in this study, the deformation values of the samples tested in the cyclic simple shear test (CSST) device under different deformation conditions were chosen as single amplitude 2%, 3.5% and 5%. Physical properties of the sand used in the experiments are given in Table 1, and the grain distribution chart is given in Fig. 4. The specific gravity of the sand given in Table 1 was determined according to

Table 2 Experimental results

Test No	σ_v (kPa)	u_0 kPa)	σ_v' (kPa)	Dr (%)	γ (%)	W (J/m^3)
1	50	25	25	40	2	803
2	100	50	50	40	2	895
3	200	100	100	40	2	2240
4	300	150	150	40	2	2804
5	50	25	25	40	3.5	575
6	100	50	50	40	3.5	1163
7	200	100	100	40	3.5	1860
8	300	150	150	40	3.5	2774
9	50	25	25	40	5	891
10	100	50	50	40	5	1402
11	200	100	100	40	5	2285
12	300	150	150	40	5	3851
13	50	25	25	55	2	891
14	100	50	50	55	2	1415
15	200	100	100	55	2	2779
16	300	150	150	55	2	4211
17	50	25	25	55	3.5	949
18	100	50	50	55	3.5	1868
19	200	100	100	55	3.5	3304
20	300	150	150	55	3.5	4114
21	50	25	25	55	5	1446
22	100	50	50	55	5	2423
23	200	100	100	55	5	3275
24	300	150	150	55	5	5090
25	50	25	25	70	2	1149
26	100	50	50	70	2	2313
27	200	100	100	70	2	4389
28	300	150	150	70	2	10864
29	50	25	25	70	3.5	1175
30	100	50	50	70	3.5	3856
31	200	100	100	70	3.5	5800
32	300	150	150	70	3.5	9462
33	50	25	25	70	5	1860
34	100	50	50	70	5	3288
35	200	100	100	70	5	5571
36	300	150	150	70	5	10877

Dr: Relative density (%), σ_v' :Vertical effective stress (kPa), σ_V:Vertical stress (kPa), u_0: Pore water pressure (kPa), γ: Shear strain (%), W: Energy per unit volume (J/m^3)

ASTM D854 and the sieve analysis was determined according to ASTM D6913.

ASTM D4253 and ASTM D4254 standards were used to determine the maximum and minimum void ratios of the sand. The specimens prepared for the experiment were 100 mm in diameter and their heights are were 46 mm. The red table shown in Fig. 2 is free to move during the test at the applied unit deformation amplitude. Due to this movement, shear stresses are applied to the sample in the mould. These shear strains lead to the rearrangement of sand particles and the development of excess pore water pressure. Sand samples are found in the mould bounded laterally by teflon-coated rings arranged around the latex membrane as shown in Fig. 5. The Teflon rings around the mould and the clamps on the top and bottom of the mould prevent the formation of balloon in the membrane due to excess pore water pressure during the test and the application of a pore water pressure to the sample before testing.

Relative density of sand specimens desired for a cyclic simple shear test can be prepared by using slurry deposition, moist tamping, or air pluviation methods (Kuerbis and Vaid 1998). In this study, the desired relative density values of sand specimens were achieved using the air pluviation method. In this method, the required sand amount was drop from a specific height (Walker and Whitaker 1967). As a result of this process, care is taken to ensure that the specimen height is always the same (46 mm). The sample height is found by measuring the height of the piston from the bottom of the sample, which allows the application of vertical stress to the sample. This is done automatically by the instrument software.

In order to ensure that the specimens prepared at the desired density are fully saturated, and to prevent air bubbles from remaining in the specimen, CO_2 is flushing from bottom to top for 20 min. After flushing with CO_2, saturation of the specimen is ensured by supplying water from bottom to top, with the water under reduced pressure from the water de-aeration system.

The de-aerated water of at least 5 times the volume of the specimen is then passed through the specimen.

After the saturation process is completed, the determined vertical stress and pore water pressures (given in Figure 3) are gradually applied to the specimen. In gradual application, the first half of the total vertical stress (σ_V) is applied to the specimen; then, half of the pore water pressure (u_0) is applied to the specimen, and then the vertical stress is increased again, and the aimed total vertical stress and pore water pressure are achieved by repeating these processes. However, targeted effective stress (σ_v')value was never exceeded during these processes. At that point, consolidation of the specimen was ensured under vertical stress and pore water pressure.

During cyclic loading, although it is less than the typical earthquake frequency, uniform sinusoidal horizontal (GDS 2006) shear stress with frequency of 0.1 Hz was applied, as is recommended for this type of test instrument. Excess pore water pressures developed during the experiments were measured using sensitive pressure sensors located below and above the specimen. All parameters during the test were automatically recorded in the experiment document as 20 per cycle, by the software of the cyclic simple shear test device. In the experiments, the specimen was assumed to be liquefied when

excess pore water pressure equivalent to starting effective vertical stress was formed. The results of all the tests carried out in this study and the initial test conditions are given in Table 2.

3. Experimental results and discussion

The tests conducted within the scope of this study were carried out using strain-controlled cyclic simple shear test under undrained conditions, as mentioned in previous sections. Figs. 6-10 show the results of a typical experiment, which was carried out within the scope of the study and whose effective stress value was 100 kPa, relative density was 70%, and shear strain was 2%. In this experiment, the number of cycles versus 2% shear strain applied to the sample are shown in Fig. 6. Shear strain amplitude is applied constantly from start to end of the experiment in strain-controlled experiments. The hysteresis loop, showing the variation of this test's shear stress according to shear strain, is given in Fig. 7. Because of the applied shear strain, excess pore water pressure in the specimen had increased until it was equivalent to vertical effective stress, and excess pore water pressure stopped when the number of cycles was approximately 7 and the specimen was liquefied. As also seen in Fig. 7, secant shear module decreases with the increase of the number of cycles. The reason for this decrease is the increase in excess pore water pressure. When liquefaction occurs, the area of the hysteresis loop is reduced too much, and the loop becomes almost flat.

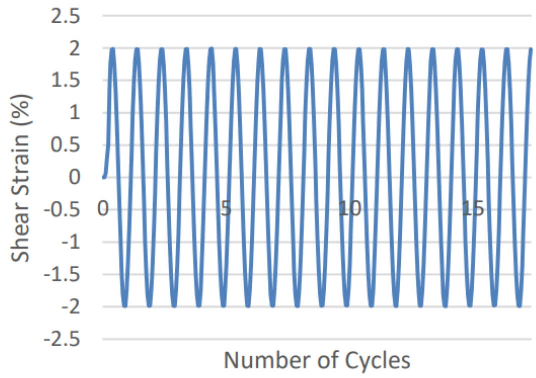

Fig. 6 Shear strain versus number of cycles at strain amplitude of 2%

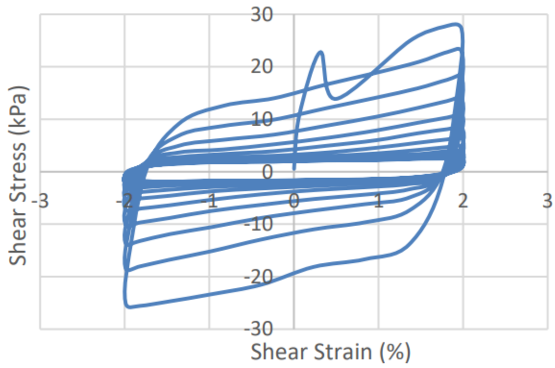

Fig. 7 The hysteresis loops

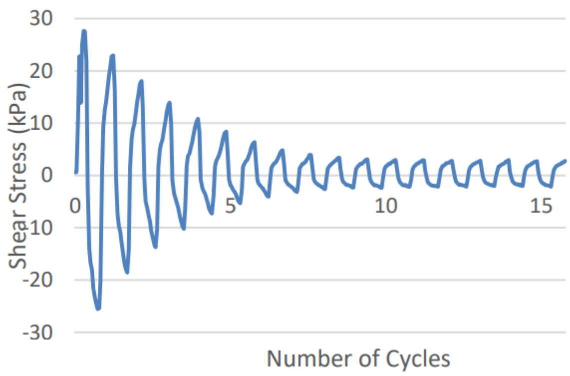

Fig. 8 Cyclic shear stress variation versus the number of cycles for γ=%2 and σ′$_v$ = 100 kPa

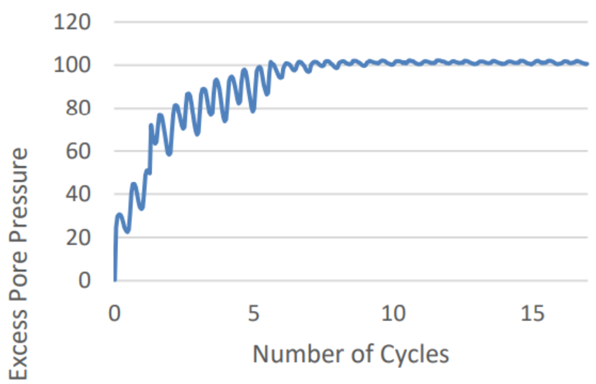

Fig. 9 Excess pore pressure versus number of cycles for γ= %2 and σ'_v = 100 kPa

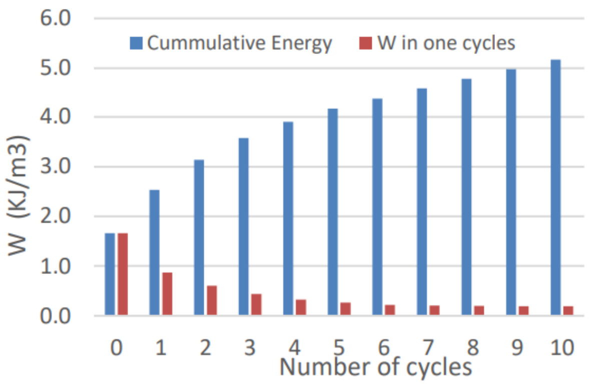

Fig. 10 Histogram of the energy dissipated per unit volume and the cumulative energy after each cycle

In Fig. 8, the variation is given of shear stress of the test mentioned above, according to number of cycles. Because of the decrease in the soil resistance as it reaches closer to liquefaction (due to the applied controlled shear strain), shear stress decreases and eventually reaches a fixed amount. It is not exactly zero, as it is theoretically in a liquid.

It is thought to be caused by a friction that exists in the test system. The variation of excess pore water pressure, according to a number of cycles, is given in Fig. 9. Under cyclic loading conditions, the shear stresses on the soil force the sand grains to resettle to a denser form. For this reason, soil tends to decrease in volume. However, this volume cannot be reduced because the soil is saturated with water and is not compressible in water, and the stresses acting on the soil are transferred to the pore water. This causes an increase in pressure in the pore water. The size of the evolving pore water pressure at this time varies according to the response to the volume reduction of the soil grain. In such conditions where there is no drainage, the excess pore water pressure increases to become equal to the effective stress and the soil loses its strength. As the density of the soil decreases, the increase in the pressure of the pore water becomes very rapid and large deformations occur. In Figure 9, due to an increase in specimen strain and denser re-settle of sand grains, the excess pore water pressure which is one of the most important indicators of soil liquefaction rapidly increases until it is equivalent to vertical effective stress and follows a horizontal course along with liquefaction.

Studies have shown that the cumulative energy causing liquefaction is a perfect index for evaluating liquefaction potential. Accordingly, various studies have been carried out to examine this parameter (Baziar and Jafarian 2007, Liang 1995). The variations of dissipated energy in each cycle and dissipated cumulative energy, depending on the increased number of cycles, are given in Figure 10. As the number of cycles increases, the cumulative energy increases, while the energy dissipated for the liquefaction of the specimen decreases.

In Fig. 10, the dissipated energy reaches the lowest level, approximately at the 7th cycle. In this case, pore water pressure becomes equivalent to effective stress (as seen in Fig. 9), shear stress applied to the specimen decreases (as seen in Fig. 8), and it reaches a fixed value. This is due to the disappearance of shear resistance of the specimen. The dissipated energy reaches the lowest level at this point, in which pore water pressure is equivalent to effective stress and the soil is liquefied. These observations show that energy dissipated per unit volume for liquefaction is related to the increase of pore water pressure.

Fig. 11 shows the variation of the liquefaction energies according to the number of cycles for the %40, %55, %70 relative density values at 100 kPa effective stress and 3.5% shear strain. The fact that relative density is an appropriate parameter for comparison in the soil liquefaction analyses has also been indicated in other studies (Hazirbaba and Rathje 2009, Carraro *et al.* 2009). As expected, with the increase of relative density, the energy required for the liquefaction of soil also increases.

However, the dissipate energy for liquefaction increases markedly with increasing relative density when comparing the energy difference between 40% and 55% relative density and the energy difference between 55% and 70% relative density. The variation of the same experiment's liquefaction energy, according to effective stress, is given in Fig. 12. It has been observed that liquefaction energy considerably increases along with the increased relative density and increased effective stress. This observation has shown that liquefaction energy strongly depends on relative density. However, the dissipate energy for liquefaction increases markedly with increasing relative density when comparing the energy difference between 40% and 55% relative density and the energy difference between 55% and 70% relative density.

The variation of the same experiment's liquefaction energy, according to effective stress, is given in Figure 12. It has been observed that liquefaction energy considerably increases along with the increased relative density and increased effective stress. This observation has shown that liquefaction energy strongly depends on relative density.

Fig. 13 shows the variation of liquefaction energy at different shear strain amplitudes of the sand specimens under 55% relative density and 100 kPa effective stress, according to number of cycles. As seen in Figure 13, the number of cycles decreases with increasing unit deformation. This reduction is further accelerated by an increase in unit deformation. However, the change in cumulative liquefaction energy is less compared to relative density and effective stress. This result shows a similarity to

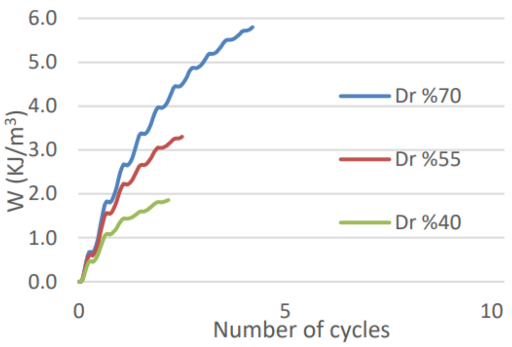

Fig. 11 Variation of cumulative liquefaction energies of specimens with different relative density according to the number of cycles for γ= %3.5 and σ′$_v$ = 100 kPa

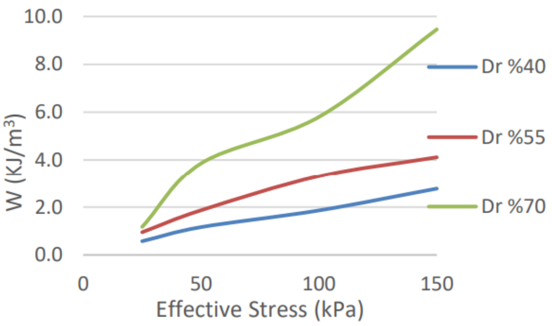

Fig. 12 Variation of cumulative liquefaction energies of specimens with different relative density according to effective stress for γ= %3.5

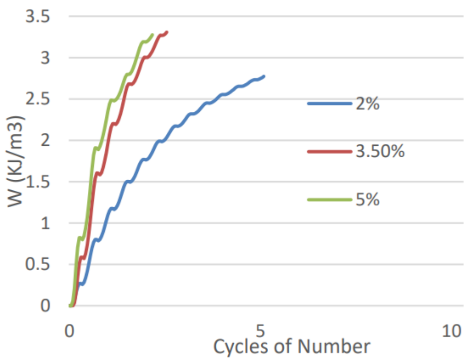

Fig. 13 Variation of cumulative liquefaction energies of specimens at different strain amplitudes according to the number of cycles for D_r=%55 and σ′$_v$ = 100 kPa

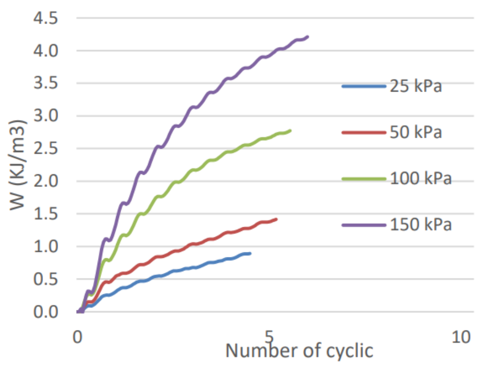

Fig. 14 Variation of cumulative liquefaction energies of specimens under different effective stresses according to the number of cycles for γ= %2 and Dr=%55

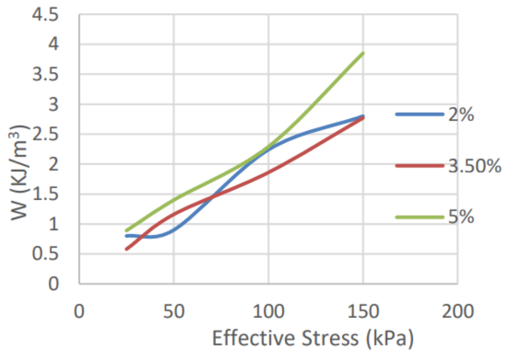

(a)

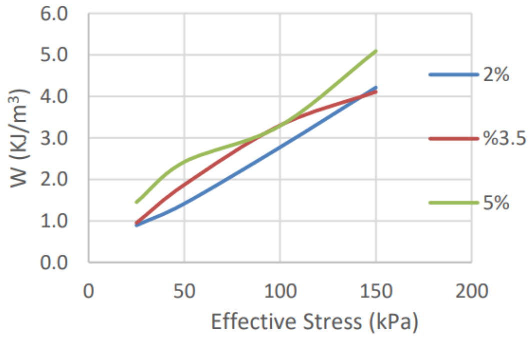

(b)

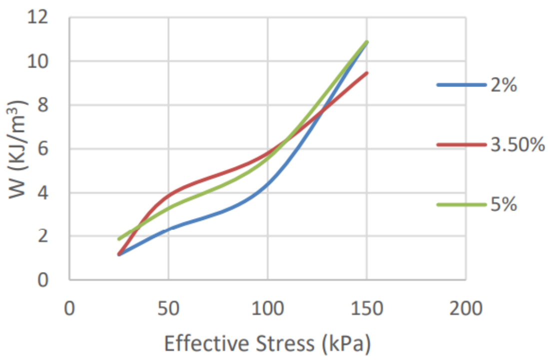

(c)

Fig. 15 (a) Variation of liquefaction energies of the samples in different unit deformation according to effective stress in (a) relative density %40, (b) in relative density %55 and (c) in relative density %70

the findings of Figuera (1994).

In Fig. 14, the variation is given for different effective stress values of the sand specimen at 2% shear strain and 55% relative density, according to the number of cycles of liquefaction energy. As can be seen in the figure, cumulative liquefaction energy increases significantly with increasing effective stress values and a slight increase in the number of cycles. When this situation is evaluated in terms of ground conditions in the field, the effective stress increases with increasing depth. Cumulative liquefaction with increased effective stress will increase in energy. Such an increase will complicate liquefaction of the deeper layers.

Figs. 15(a), 15(b) and 15(c) give the variation of liquefaction energies of specimens at different relative density (40, 55, 70%) values, according to effective stress different shear strain amplitudes. Along with increased relative density and increased effective stress, the liquefaction energies increase at all shear strain amplitudes.

However, as mentioned in the previous paragraph the liquefaction energy is less affected by the change in the shear unit deformation amplitude compared to the relative density and effective stress. This effect is usually due to a limited increase in the liquefaction energy as the amplitude of the unit deformation increases. This shows that the liquefaction energy is less dependent on the shear deformation amplitude. However, as the relative density and effective stress increases, the difference between the cumulative liquefaction energies in different unit deformations becomes more pronounced. These results were obtained in other studies (Figueroa *et al.* 1994, Liang 1995).

3.1 Regression analyses

As a result of the tests carried out in this study, the effects of effective stress, relative density, and shear strain are shown with the information and graphs given in previous sections. A generalized relationship has been obtained between the mentioned factors and the liquefaction energy dissipated per unit volume. For this purpose, a multiple regression analysis was performed between the mentioned factors and the liquefaction energy per unit volume. In this study, liquefaction energy per unit volume is the dependent variable, and effective stress, relative density, and shear strain are the independent variables. The relationship with the highest correlation coefficient (R^2=0.95) obtained from the analyses is given in Eq. (2).

$$W(J/m^3) = \exp(0.0123\sigma_v' + 0.0412D_r + 0.0397\gamma + 4.33) \quad (2)$$

where; W: Liquefaction energy per unit volume (J/m3), σ'_v: Vertical effective stress (kPa), Dr: Relative density (%), γ: Shear strain amplitude (%)

The relationship between the liquefaction energy obtained as a result of the study and the liquefaction energy determined by using the relationship obtained from the regression analysis is given in Fig. 16.

As indicated previously, shear strain amplitudes were chosen as 2, 3.5, and 5% in the experiments carried out in this study. However, previous sections have shown the fact that shear strain is less effective on the test results, compared to relative density and effective stress. In this section, the regression analysis was carried out between liquefaction energies per unit volume obtained from the experiments by only two variable parameters relative density and effective stress instead of three variable parameters. As a result of the analysis, a high correlation (R^2=0.94) was obtained between the mentioned parameters and the liquefaction energy. The relationship obtained as a result of the analysis is given in Eq. (3). When equation 3 (in which the effect of shear strain is absent) is compared with Eq. (2), the difference between correlation coefficients is only 0.01. In this case, it can be concluded that the effect of shear strain is negligible in the calculation of liquefaction energy per unit volume.

It is recommended to prefer the relationship given in Eq. (3), due to its simplicity in calculating liquefaction energy and to its high correlation coefficient. The relation between the liquefaction energy per unit volume obtained from Eq.

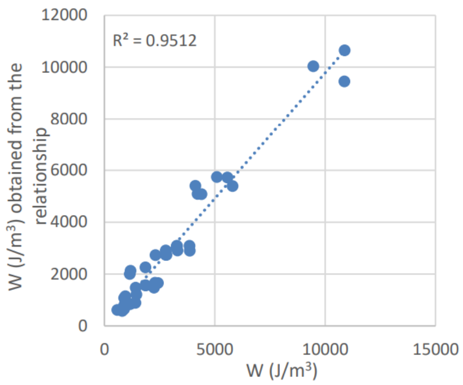

Fig. 16 The relation between test results and the results obtained from the relationship

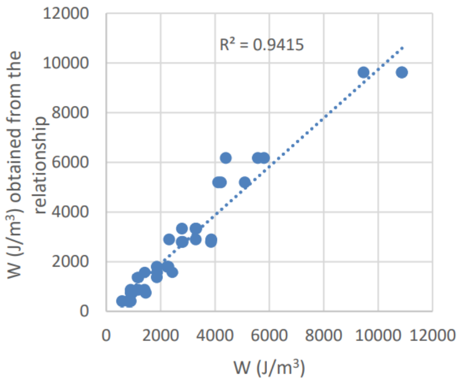

Fig. 17 The relation between test results and the results obtained from the relationship

Table 3 Equations providing liquefaction energy per unit volume in the literature

Figuera vd. (1994)	$Log(W) = 2.002 + 0.00477\sigma'_{mean} + 0.0116D_r$	R^2=0.94
Liang (1995)	$Log(W) = 2.062 + 0.0039\sigma'_{mean} + 0.0124D_r$	R^2=0.92
Rokoff (1999)	$Log(W) = 1.371 + 0.00597\sigma'_{mean} + 0.02067D_r$	R^2=0.87
Dief and Figuera (2001)	$Log(W) = 1.164 + 0.0124\sigma'_{mean} + 0.0209D_r$	R^2=0.94
Jafarian (2012)	$W = 0.1363P_0'(\frac{D_r}{100})^{4.925} + 5.375 \times 10^{-3} \times P_0'$	R^2=0.8
This study	$W = 2.248 + (\sigma_v')^{1.094} \times (1.042)^{D_r}$	R^2=0.94

W: Liquefaction energy per unit volume; (J/m3), σ'_{mean}, P'_0 = Effective mean confining pressure (kPa),Dr= Relative density (%), σ'_v: Vertical effective stress (kPa)

(3) and the liquefaction energy obtained from test results is given in Fig. 17.

$$W = 2.248(\sigma_v')^{1.094}(1.042)^{Dr} \quad (3)$$

Some of the relations suggested in the studies based on energy in the literature are given in Table 3. Figuera *et al.* (1994) performed 27 strain controlled tests on reid bedford sand using hollow cylinder torsional shear test. In another study, Liang (1995) performed 9 strain controlled tests on reid bedford sand using hollow cylinder torsional shear test.

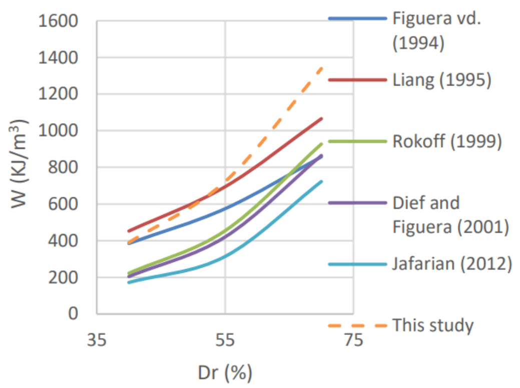

Fig. 18 Liquefaction energies at different relative density values under effective stress of 25 kPa

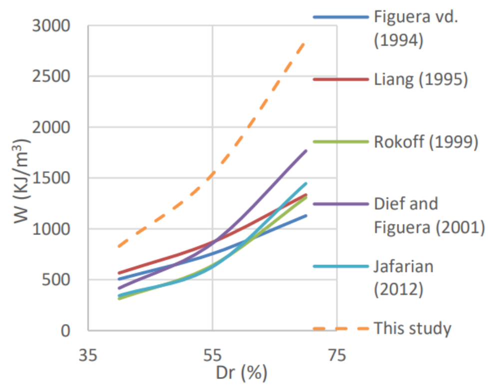

Fig. 19 Liquefaction energies at different relative density values under effective stress of 50 kPa

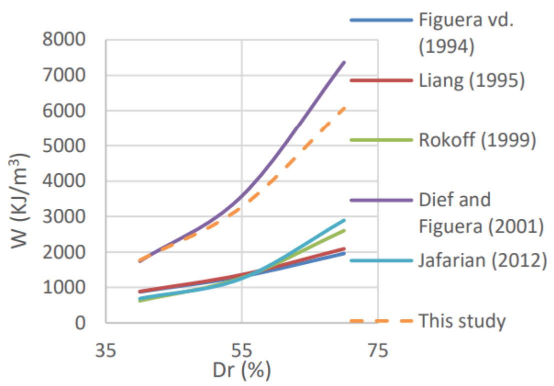

Fig. 20 Liquefaction energies at different relative density values under effective stress of 100 kPa

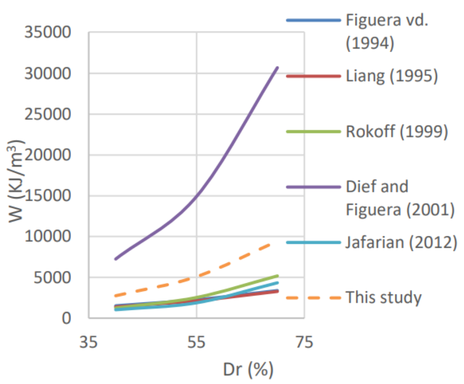

Fig. 21 Liquefaction energies at different relative density values under effective stress of 150 kPa

Moreover, Rokoff (1999) performed strain controlled tests on Neveda sand using hollow cylinder torsional shear test. Dief and Figuera (2001) conducted 20 tests on Reid Bedford and Neveda sands using the centrifuge test. Finally, Jafarian *et al*. (2012) performed 37 tests on sand using hollow cylinder using both torsinal shear tests and cyclic simple shear tests. The results of the relationship proposed in this study are compared to the results of relationships proposed in studies previously carried out and which are given in Table 3, and the results are given in Figs. 18-21.

When the studies were examined, it was found that relationships were mainly derived by using the results of hollow cylinder torsional shear tests. However, in liquefaction tests, the author is not aware of a relationship that provides liquefaction energy per unit volume, derived by only using a cyclic simple shear test that models the dynamic loading conditions of the soil in the field, compared to other test instruments. For this reason, the relationship derived from this study is important, because it is the first equation to be derived by using only the results of the cyclic simple shear test.

In Fig. 18, liquefaction energies are given comparatively for different relative densities under 25 kPa effective stress. As seen in the figure, while the results of the relationships proposed in other studies yield quite compatible values with the results of the equation proposed in this study at low relative density values, the results of other studies vary from the results of this study with increasing relative density, and they yield lower energy values. In all effective stress values of Figs. 19-21, liquefaction energies increase in all relationship results with the increase of relative density. However, the results of the relationship proposed by Dief and Figuera (2001) vary considerably from the results of the equations proposed in this study (and other studies) as effective stress value increases and it yields high liquefaction energy values. The results of relationships proposed in the studies carried out by Figuera *et al.* (1994), Liang (1995), Rokoff (1999), and Jafarian *et al.* (2012) yield lower energy values than the results of the relationship proposed in this study, at all relative density and effective stress values.

Since liquefaction energy is less dependent on shear strain, it is possible to calculate liquefaction energy per unit volume by determining relative density and effective stress values in a field. Relative density of a soil layer can be determined by using familiar tests in the field (SPT, CPT). Vertical effective stress, affecting a soil layer at a certain depth, is the multiplication of unit volume weight of the soil and depth, and it can be easily calculated. In such cases, the energy required for the layer to be liquefied can be determined by using Eq. (3). If one can calculate the energy that a possible earthquake can apply on layers of the soil, one can determine whether or not those layers can be liquefied.

The hollow cylinder torsional shear test was used more in the studies mentioned above. However, in the technical report prepared by Kammerer and Pestana (2002), it is reported that the soils tested in the hollow cylinder torsional shear test instrument are less resistant to liquefaction than the same soils tested on the cyclic simple shear tester from time to time. The less resistance of the sample to liquefaction means less liquefaction energy. In addition, the soil fabric, the surface roughness of the grains and the sample preparation method also might decrease this liquefaction energy.

4. Conclusions

An energy-based approach to identify the liquefaction potential of soils per unit volume is presented. This approach has the ability to represent the onset of the liquefaction of the undrained soil layer with an amount of energy during dynamic motion.

According to the results obtained from the experiments, liquefaction energy per unit volume increases with increased effective stress at all relative density values used in this study, similar to previous studies. At all shear strain amplitudes, the liquefaction energy per unit volume increases with the increase of effective stress and relative density; however, this increase in liquefaction energy is less affected by the increase of shear strain amplitude. In other words, liquefaction energy yields the same values under the same relative density and effective stress, but at different shear strain amplitudes. This is a strong indication that liquefaction energy is less dependent on shear deformation amplitude. Since the energy in a unit volume required for liquefaction is less dependent of shear strain amplitude, this shows that an energy-based approach can be used for non-uniform shear strain amplitudes, such as an earthquake in actual field conditions.

The relationship proposed in this study is important, since it is the first energy-based relationship derived only from the results of a cyclic simple shear test. However, the correlation here is valid for the physical properties of the sand given in the previous sections in terms of relative density (%40, 55, 70) effective stress (25, 50, 100, 150 kPa) and shear strain (%2, 3.5, 5). While the results of other relationships in the literature yield fairly compatible liquefaction energy values at low effective stress values, and low relative density values compared to the results of the relationship proposed in this study, they yield lower energy values with increased relative density. At high effective stress values, they yield lower energy values than the results of the relationship given in this study, both at high relative density and at low relative density. Since liquefaction energy per unit volume is less dependent of shear strain amplitude, the relationship proposed in this study can be used in calculating the required energy for the liquefaction of soil. In addition, this calculated energy can be used to predict if a field can be liquefied or not, by comparing it with the energy per unit volume to be transferred to the soil, due to dynamic energy to be produced by a potential earthquake in the field.

Acknowledgements

This research was funded by Kirikkale University under grant number 2018/021. Experiments were carried out in the Soil Mechanics Laboratory of Ankara University. Dr. Kamil Kayabali kindly provided access to this laboratory.

References

Alavi, A.H. and Gandomi, A.H. (2012), "Energy-based numerical models for assessment of soil liquefaction", *Geosci. Front.*, **3**(4), 541-555.

ASTM D854-14 (2018), *Standard Test Methods for Specific Gravity of Soil Solids by Water Pycnometer*, Annual Book of ASTM Standards, ASTM International.

ASTM D4253-16 (2018), *Standard Test Methods for Maximum Index Density and Unit Weight of Soils Using a Vibratory Table*, Annual Book of ASTM Standards, ASTM International.

ASTM D4254-16 (2018), *Standard Test Methods for Minimum Index Density and Unit Weight of Soils and Calculation of Relative Density*, Annual Book of ASTM Standards, ASTM International.

ASTM D6913 (2018), *Standard Test Methods for Particle-Size Distribution (Gradation) of Soils Using Sieve Analysis*, Annual Book of ASTM Standards, ASTM International.

Baziar, M.H. and Jafarian, Y. (2007), "Assessment of liquefaction triggering using strain energy concept and ANN model capacity energy", *Soil Dyn. Earthq. Eng.*, **27**(12), 1056-1072.

Baziar, M.H. Jafarian, Y. Shahnazari, H. Movahed, V. and Tutunchian, M.A. (2011), "Prediction of strain energy-based liquefaction resistance of sand-silt mixtures: An evolutionary approach", *Comput. Geosci.*, **37**(11), 1883-1893.

Berrill, J.B. and Davis, R.O. (1985), "Energy dissipation and seismic liquefaction of sands: revised model", *Soil. Found.*, **25**(2), 106-118.

Bjerrum, L. and Landva, A. (1966), "Direct simple shear tests on a Norwegian quick clay", *Geotechnique,* **16**(1), 1-20.

Boulanger, R.W. and Idriss, I.M. (2012), "Probabilistic standard penetration test-based liquefaction-triggering procedure", *J. Geotech. Geoenviron. Eng.*, **138**(10), 1185-1195.

Carraro, J.A.H., Prezzi, M. and Salgado, R. (2009), "Shear strength and stiffness of sands containing plastic or nonplastic fines", *J. Geotech. Geoenviron. Eng.*, **135**(9), 1167-1178.

Cetin, K.O., Seed, R.B., Der-Kiureghian, A., Tokimatsu, K., Harder Jr, L.F., Kayen, R.E. and Moss, R.E.S. (2004), "Standard penetration test-based probabilistic and deterministic assessment of seismic soil liquefaction potential", *J. Geotech. Geoenviron. Eng.*, **130**(12), 1314-1340.

Chang, W.J. and Hong, M.L. (2008), "Effects of clay content on liquefaction characteristics of gap-graded clayey sands", *Soil. Found.*, **48**(1),101-114.

Chen, Y.R. Hsieh, S.C. Chen, J.W. and Shih, C.C. (2005), "Energy-based probabilistic evaluation of soil liquefaction", *Soil Dyn. Earthq. Eng.*, **25**(1), 55-68.

Cubrinovski, M. Bradley, B.A. Wotherspoon, L., Green, R., Bray, J., Wood, C., Pender, M., Allen, J., Bradshaw, A., Rix, G., Taylor, M., Robinson, K., Henderson, D., Girorgini, S., Ma, K., Winkley, A., Zupan, J., O'Rourke, T., DePascale, G. and Wells, D. (2011), "Geotechnical aspects of the 22 February 2011 Christchurch earthquake", *Bull. N. Z. Soc. Earthq. Eng.*, **44**, 205-226.

DeAlba, P., Seed, H.B. and Chan, C.K. (1976), "Sand liquefaction in large-scale simple shear tests", *J. Geotech. Geoenviron. Eng.*, **102**(GT9), 909-927.

Dief, H.M. and Figueroa, J.L. (2001), "Liquefaction assessment by the energy method through centrifuge modeling", *Proceedings of the NSF International Workshop on Earthquake Simulation in Geotechnical Engineering*, Cleveland, Ohio, U.S.A., July,

Dobry, R., Ladd, R., Yokel, F., Chung, R. and Powell, D. (1982), "Prediction of pore water pressure buildup and liquefaction of sands during earthquakes by the cyclic strain method", National Bureau of Standards Building Science Series 138, US Department of Commerce, U.S.A.

Dyvik, R., Berre, T., Lacasse, S. and Raadim, B. (1987), "Comparison of truly undrained and constant volume direct simple shear tests", *Geotechnique*, **37**(1), 3-10.

Fardad, A.P. and Noorzad, R. (2018), "Energy-based evaluation of liquefaction of fiber-reinforced sand using cyclic triaxial testing", *Soil Dyn. Earthq. Eng.*, **104**, 45-53.

Figueroa, J., Saada, A., Liang, L. and Dahisaria, N. (1994), "Evaluation of soil liquefaction by energy principles", *J. Geotech. Eng.*, **120**(9), 1554-1569.

GDS (2006), *Equipment User Manual*, GDS Corporation, U.K.

Green, R.A. (2001), "Energy-based Evaluation and Remediation of Liquefiable Soils", Ph.D. Dissertation, Virginia Polytechnic Institute and State University, Blacksburg, Virginia, U.S.A.

Hazirbaba, K. and Rathje, E.M. (2009), "Pore pressure generation of silty sands due to induced cyclic shear strains", *J. Geotech. Geoenviron. Eng.*, **135**(12), 1892–1905.

Ishihara, K. (1985), "Stability of natural deposits during earthquakes", *Proceedings of the 11th International Conference on Soil Mechanics and Foundation Engineering*, San Francisco, California, U.S.A., August

Ishihara, K. and Yasuda, S. (1975), "Sand liquefaction in hollow cylinder torsion under irregular excitation", *Soil. Found.*, **15**(1), 45-59.

Jafarian, Y. Towhata, I. Baziar, M.H. Noorzad, A. and Bahmanpour, A. (2012), "Strain energy based evaluation of liquefaction and residual pore water pressure in sands using cyclic torsional shear experiments", *Soil Dyn. Earthq. Eng.*, **35**, 13-28.

Jafarzadeh, F. and Sadeghi, H. (2012), "Experimental study on dynamic properties of sand with emphasis on the degree of saturation", *Soil Dyn. Earthq. Eng.*, **32**(1), 26-41.

Kammerer, A. and Pestana, J.M. (2002), "Undrained response of Monterey 0/30 sand under multidirectional cyclic simple shear loading conditions", Technical report University of California, Berkeley, California, U.S.A.

Kokusho, T. (2013), "Liquefaction potential evaluation: Energy-based method comparedto stress-based method", *Proceedings of the 7th International Conference on Case Histories in Geotechnical Engineering*, Chicago, Illinois, U.S.A., April-May.

Kuerbis, R. and Vaid, Y.P. (1998), "Sand sample preparation: The slurry deposition method", *Soil. Found.*, **28**, 107-118.

Law, K.T. Cao, Y.L. and He, G.N. (1990), "An energy approach for assessing seismic liquefaction potential", *Can. Geotech. J.*, **27**(3), 320-329.

Liang, L. (1995) "Development of an energy method for evaluating the liquefaction potential of a soil deposit", Ph.D. Dissertation, Case Western Reserve University, Cleveland, Ohio, U.S.A.

Monkul, M.M. Gultekin, C. Gulver, M. Akın, O. and Eseller-Bayat, E, (2015), "Estimation of liquefaction potential from dry and saturated sandy soils under drained constant volume cyclic simple shear loading", *Soil Dyn. Earthq. Eng.*, **75**, 27-36.

Moss, R.E.S., Seed, R.B., Kayen, R.E., Stewart, J.P., Der Kiureghian, A. and Cetin, K.O. (2006), "CPT based probabilistic and deterministic assessment of in situ seismic soil liquefaction potential", *J. Geotech. Geoenviron. Eng.*, **132**(8), 1032-1051.

Nemat-Nasser S. and Shokooh A. (1979), "A unified approach to densification and liquefaction of cohesionless sand in cyclic shearing", *Can. Geotech. J.*, **16**(4), 659-678.

Ostadan, F., Deng, N. and Arango, I. (1996), *Energy-Based Method for Liquefaction Potential Evaluation*, *Phase I. Feasibility Study*, U.S. Department of Commerce, Technology Administration, National Institute of Standards and Technology, Building and Fire Research Laboratory, Gaithersburg, Maryland, U.S.A.

Polito, C., Green, R.A., Dillon, E. and Sohn, C. (2013), "Effect of load shape on relationship between dissipated energy", *Can. Geotech. J.*, **50**(11), 1118-1128.

Rokoff, M.D. (1999), "The influence of grain-size characteristics in determining the liquefaction potential of a soil deposit by the energy method", M.Sc. Thesis, Case Western Reserve University, Cleveland, Ohio, U.S.A.

Seed, H.B. (1980), "Closure to soil liquefaction and cyclic mobility evaluation for level ground during earthquakes", *J. Geotech. Eng.*, **106**(6), 724.

Seed, H.B. and Idriss, I.M. (1971), "Simplified procedure for evaluating soil liquefaction potential", *J. Soil Mech. Found.*, **97**(8), 1249-1274.

Seed, H.B. and Lee, K.L. (1967), "Undrained strength characteristics of cohesionless soils", *J. Soil Mech. Found. Div.*, **93**(SM6), 333-360

Seed, H.B. Idriss, I.M., Makdisi, F. and Banerjee, N. (1975), "Representation of irregular stress time histories by equivalent uniform stress series in liquefaction analyses", Report No. UCB/EERC-75/29, Earthquake Engineering Research Centre, University of California, Berkeley, California, U.S.A.

Silver, L.M. and Park, T.K. (1976), "Liquefaction potential rvaluated from cyclic strain-controlled properties tests on sands", *Soil. Found.*, **16**(3), 51-65.

Simcock, J., Davis, R.O., Berrill, J.B. and Mallenger, G. (1983), "Cyclic triaxial tests with continuous measurement of dissipated energy", *Geotech. Test. J.*, **6**(1), 35-39.

Talaganov, K.V. (1996), "Stress-strain transformation and liquefaction of sand", *Soil Dyn. Earthq. Eng.*, **15**(7), 411-418.

Towhata, I. (2008), *Geotechnical Earthquake Engineering*, Springer-Verlag Berlin and Heidelberg GmbH & Co. KG, Berlin, Germany.

Towhata, I. and Ishihara, K. (1985), "Shear work and pore water pressure in untrained shear", *Soil. Found.*, **25**(3), 73-84.

Walker, B.P. and Whitaker, T. (1967), "An apparatus for forming beds of sands for model foundation tests", *Geotechnique*, **17**(2), 161-167.

Wijewichreme, D. Sriskandakumar, S. and Byrne, P.M. (2005), "Cyclic loading response of loose air-pluviated Fraser River sand for validation of numerical models simulating centrifuge tests", *Can. Geotech. J.*, **42**(2), 41-66.

Wotherspoon, L.M., Orense, R.P. Bradley, B.A., Cox, B.R., Wood, C.M. and Green, R.A. (2015), "Soil profile characterization of Christchurch central business district strong motion stations", *Bull. N. Z. Soc. Earthq. Eng.*, **48**(3), 147-157.

Youd, T.L. and Idriss I.M. (2001), "Liquefaction resistance of soils: summary report from the 1996 NCEER and 1998 NCEER/NSF workshops on evaluation of liquefaction resistance of soils", *J. Geotech. Geoenviron. Eng.*, **127**(4), 297-313.

Zaheer, A.A., Kamran, A. and Naeem, A.M. (2013), "Liquefaction Potential of Silty Sand in Simple Shear", *Mehran Univ. Res. J. Eng. Technol.*, **32**(1), 85-94.

Zhang, W. and Goh, A.T.C. (2016), "Evaluating seismic liquefaction potential using multivariate adaptive regression splines and logistic regression", *Geomech. Eng.*, **10**(3), 269-284.

Zhang, W. Goh, A.T.C., Zhang, Y., Chen, Y. and Xiao, Y. (2015), "Assessment of soil liquefaction based on capacity energy concept and multivariate adaptive regression splines", *Eng. Geol.*, **188**, 29-37.

CC